Iterative Electrical–Thermal Coupled Simulation Method of Automotive Power Module Used in Electric Power Steering System

JANGMUK LIM[ID]1, JAEJIN JEON[ID]1, JIHWAN SEONG[ID]1, JAEHYUN CHO2, SEONG MOO CHO3, KWANG SOO KIM3, AND SANG WON YOON[ID]1, (Senior Member, IEEE)

1Department of Automotive Engineering, Hanyang University, Seoul 04763, South Korea
2Department of Automotive Engineering (Automotive-Computer Convergence), Hanyang University, Seoul 04763, South Korea
3Power Electronics Laboratory, LG Electronics Inc., Seoul 04763, South Korea

Corresponding author: Sang Won Yoon (swyoon@hanyang.ac.kr)

ABSTRACT This paper presents a multi-physics analysis coupling the electrical and thermal properties of a power module. As power modules have multi-physical behaviors, it is important to simulate their multi-physical characteristics. Simulations of these characteristics have been separately conducted using specific software; however, as these characteristics are often coupled, it is difficult to fully understand the multi-physical nature of power modules. This paper proposes a method to analyze the coupled characteristics of a power module in an iterative manner. The analyzed module is designed for an automotive electric power steering (EPS) system. We fabricated the EPS module and measured its electrical and thermal characteristics, which were used for reference. For the coupled simulation, we employed ANSYS Icepak and Q3D Extractor for thermal and electrical simulations, respectively, linked them to the ANSYS workbench environment, and conducted an iterative feedback simulation until the simulated results converged. The coupled simulation demonstrated that the parasitic resistance and volume loss density of the power module are increased by ∼50% compared to the those obtained from a separately conducted electrical simulation due to the impact of the linked thermal simulation. As a result, the simulated thermal resistance increased to 0.26 K/W, which is almost identical to the measured value of ∼0.27 K/W. Therefore, our iterative electrical–thermal coupled simulation exhibits more accurate results than the conventional separate simulations.

INDEX TERMS Electric power steering system, power module, thermal resistance, multi-physics simulation.

I. INTRODUCTION

Multi-physics analysis is important in understanding and pre-determining the performance and reliability of electrical components. A power module is a physical container of power semiconductor devices and is the core component in many electrical systems, including home appliances, industrial equipment [1], [2], power supply and transmission, renewable energy [3], and train [4] and vehicle electrifications [5]. The performance and reliability of such systems are largely determined by their multi-physical properties [6], and thus, multi-physics analyses of power modules are becoming more critical.

The associate editor coordinating the review of this manuscript and approving it for publication was Jie Gao[ID].

Figure 1 depicts a typical process of designing a power module for a target application [7], [8]. Once the design concept and required specifications are determined, the module design is conceptualized and modeled. The modeled module is preliminarily characterized by electrical, thermal, and mechanical simulations in the virtual domain. Depending on the simulation results, it is common for the module model to be modified and simulated again until the required specifications are sufficiently fulfilled. Once a satisfactory design is achieved, the module prototype is fabricated and experimentally validated in the physical domain.

The simulation procedure is one of the core steps of power module development. Generally, electrical, thermal, or mechanical simulations are conducted separately using specific software [9]–[17]. Electrical simulation software
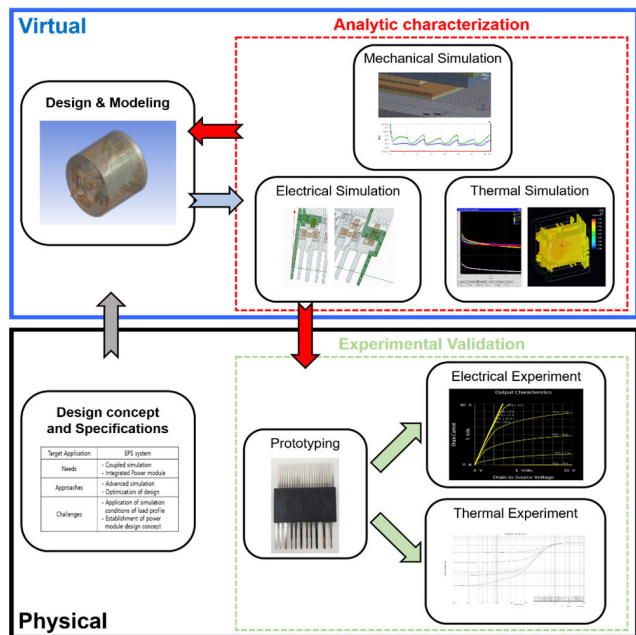
FIGURE 1. A typical development process for a power module incorporating virtual and physical domains. Mechanical simulation and experiment are not displayed because they are not included in this work.

considers electrical properties, including parasitic inductance and resistance, current density, ohmic loss density, substrate voltage, and electric field in switching devices [9]–[12]. Thermal simulation software considers temperature distribution, maximum junction temperature, thermal resistance, and cooling performance [9], [10], [13]–[15]. Mechanical simulation software considers von Mises stress, plastic strain, and deflection [13], [15]–[17]. In addition, new simulation tools with advanced models are actively being investigated for comprehensive and rapid power module simulations [18], [19].

These individual simulations are effective, but their results sometimes lead to limited performances. One reason for this is that the multi-physical characteristics of power modules are often coupled. As an example, the electrical characteristics of a power device are also influenced by its junction temperature. It has been reported that the junction temperature of a power metal-oxide-semiconductor field-effect transistor (MOSFET) changes its I–V curves and safe operating area [20], [21]. In addition, an elevated junction temperature impacts the leakage current of SiC MOSFETs and their short-circuit failure [22]. These coupled properties have been extensively studied at the device level [23], [24], but they are rarely reported in power module analyses.

Therefore, there is a strong need for a coupled multi-physics power module simulation. It is noteworthy that the coupled simulation should preferably be conducted in an iterative manner. Several previous efforts have applied the results of one simulation to the initial conditions of the following simulation. In one study, the current density derived from an electrical simulation was converted to the loss condition, which was used for thermal simulation [10], [25]. In another study, simulated running fluid in a cooler was

used to infer the heat transfer coefficient in a finite element method (FEM) thermal simulation [9]. When using such a one-time simulation without iteration, it is difficult to comprehensively understand the coupled performance and reliability of a power module. However, there has been no extensive effort to analyze the coupled phenomena of a power module using a coupled FEM simulation.

Coupled analysis with iterations has another advantage in the possibility of implementing a virtual development process (VPD). A VPD is a development strategy aimed a designing and verifying a product based on computer simulations. VPDs can improve product quality while minimizing physical prototypes and time to market.

Figure 2 illustrates the conventional development process of a power module and how the process can be improved by introducing a VPD. The conventional manner in Fig. 2(a) requires multiple re-designs using the information achieved from the prototyping and performance elevation in the physical domain, which readily leads to burdensome cost and time. However, the cost and time burden boost the necessity of the virtual-domain validation, as highlighted by the red-colored box in Fig. 2(b). As the figure shows, the iterative multi-physics simulation repeatedly validates and redesigns the virtual power module. As this repeating process is conducted in a virtual environment, significant reductions in the time and cost of prototyping and experimentally evaluating the power module prototype are expected. Thus, when a VPD process is applied, the advantages of the coupled multi-physics simulation with iteration are enhanced; in other words, these benefits are difficult to be realized without such a simulation with a (guaranteed) high accuracy.

This paper reports the development of iterative coupling electrical and thermal simulations of a self-designed power module. First, the experimental calibration of the electrical and thermal characteristics of the module are reported. The experimental results can serve as a reference for comparison with the results achieved either by (conventional) individual FEM simulations or by (our) iterative simulation coupling individual FEMs.

II. DESIGN CONCEPT AND EXPERIMENTAL CHARACTERIZATION
A. TARGET APPLICATION: AUTOMOTIVE ELECTRIC POWER STEERING (EPS) SYSTEM

The power module considered in this study was custom designed for use in automotive electric power steering (EPS) systems, providing a voltage rating of 40V and current rating of 100A. EPS systems assist the steering system using electric motors instead of existing hydraulic systems and are expected to achieve better fuel economy than traditional hydraulic power steering systems, which suffer from engine power loss from the hydraulic pressure required for power steering. Other benefits include light vehicle weight, accurate and adequate vehicle control by allowing intervention of the electronic control unit (ECU) during steering, and easy application to autonomous vehicles.
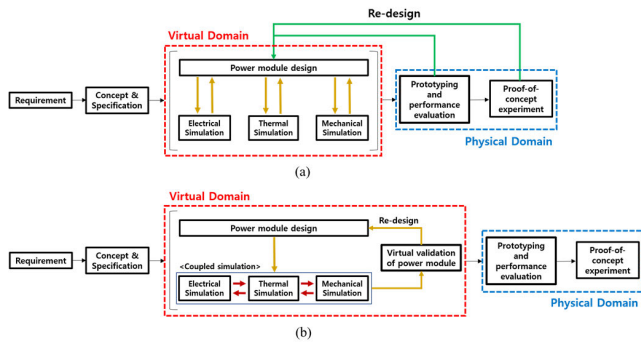
FIGURE 2. Power module development processes (a) in a conventional manner without a virtual development process (VPD) and (b) when a VPD with iterative multi-physics simulation is applied.

Available EPS systems can be largely categorized based on their motor position: rack-EPS (R-EPS), pinion-EPS (P-EPS), and column-EPS (C-EPS) [26]. R-EPS systems have a motor directly attached to the steering rack and can provide powerful and precise handling with excellent steering feel. However, the R-EPS is currently only employed in premium and luxury cars because it is expensive, space-consuming, and often exposed to high temperatures and wet environments because of its motor position. In a single pinion EPS system, the motor drives the pinion gear connecting the rack and steering shaft, resulting in a better feel than in the C-EPS type system. However, its installation is structurally complex, and the pinion gear must endure the torque transmitted to the rack. These limitations may be mitigated by employing a dual-pinion EPS system, with a secondary pinion gear added to the rack. A C-EPS system has a motor mounted on its steering column driving the steering shaft. Although C-EPS has problems including poor steering feel and limited application to small-sized vehicles, it is still attractive for mass production because of its compact size, simple construction, relative inexpensiveness, and less exposure to harsh environments. Thus, in this study, a three-phase inverter power module was designed to drive a C-EPS motor.

B. EPS POWER MODULE DESIGN

Many EPS systems employ discrete devices on a printed circuit board (PCB) [27], but there are several exceptions consisting of bare power dies soldered on a ceramic substrate, such as direct bonded copper (DBC) [28]. The ceramic substrate approach is more expensive than the PCB-based one, but it is appealing due to its superior thermal and electrical reliability (because of the substrate characteristics) and compact module size (because of the power dies) [2], [9]. To moderate the impact of the increased cost, our power module was designed using a substrate with only a top copper pattern on an insulation layer.

Figure 3(a) shows a top view of the designed power module. MOSFETs are used as the switching devices. MOSFET dies have drain-source breakdown voltage of 40V, and on-state drain current of 100A with an operating junction temperature up to 175°C [29]. There are three phases in the
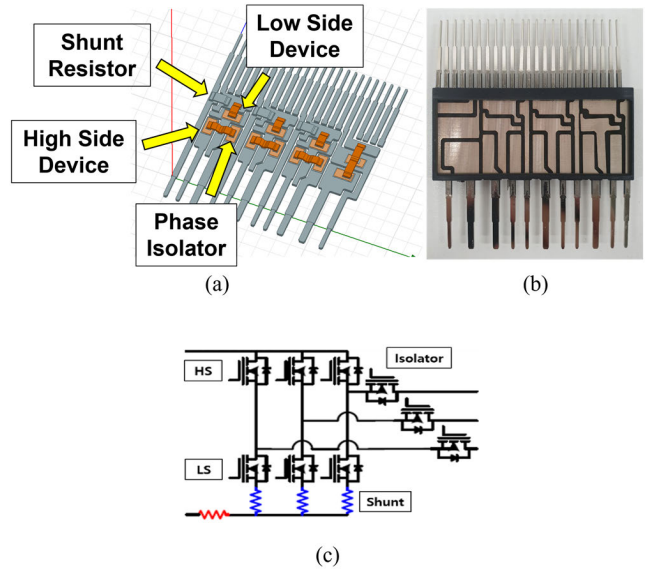

FIGURE 3. (a) Top view of the 3D model of the designed EPS power module with component notation, (b) Appearance of the fabricated power module, and (c) a circuit diagram symbolizing the designed EPS power module.
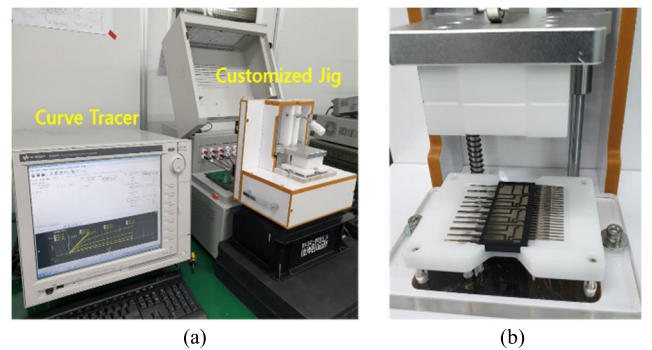

FIGURE 4. (a) Experimental setup for electrical characteristics measurement and (b) the power module under test with the customized jig.

module, and each phase consists of three MOSFETs, providing high-side and low-side switching and phase isolators. In addition, a shunt resistor is placed for each phase. The module design in Fig. 3(a) was fabricated and molded to be as shown in Fig. 3(b). Figure 3(c) shows the circuit diagram of the designed power module.

C. PERFORMANCE EVALUATION OF THE FABRICATED POWER MODULE

The electrical and thermal performances of the EPS power module were experimentally characterized. Its electrical characteristics were measured using a curve tracer (B1505A from Keysight) with a customized jig, as shown in Fig. 4.

The measurement results are plotted in Fig. 5 showing two I–V curves of $V_{GS}-I_D$ and $V_{DS}-I_D$ characteristics. The $V_{GS}-I_D$ curve shows the relationship between the input voltage (gate-source voltage, V_{GS}) and output current (drain current, I_D), while the $V_{DS}-I_D$ curve is an indicator of the ranges
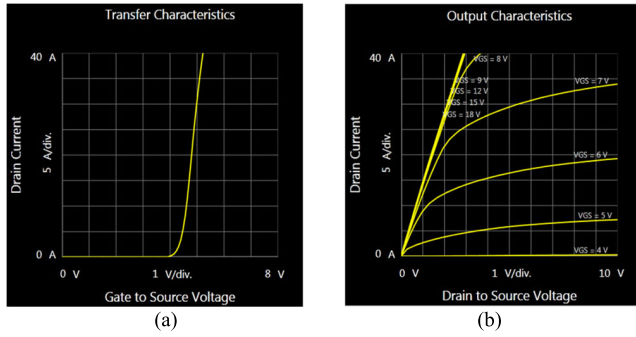
FIGURE 5. I–V curves of the (a) $V_{GS}-I_D$ and (b) $V_{DS}-I_D$ characteristics.

FIGURE 6. (a) Mentor Graphics 1500A Power Tester for thermal resistance measurement and (b) zoomed-in view of the power module under measurement.

of operating current and voltage. Both measurements are well matched with the specifications given in the MOSFET datasheet. These observations confirm that the embedded MOSFET devices function correctly and do not suffer damage or performance shifts due to module packaging. Thus, the fabricated power module samples were reliable.

Thermal resistance is an important parameter that represents the thermal performance of a power module. The thermal resistance can be simply obtained by

$$R_{th(x-y)} = \frac{T_x - T_y}{P_{loss}} = \frac{\Delta T_{x-y}}{P_{loss}} \quad (1)$$

where the device power loss, P_{loss}, generates the temperature difference, ΔT_{x-y}, between two locations x and y. The module R_{th} can be calibrated by various methods, but this work employed a method using a temperature-sensitive electrical parameters (TSEP) of the MOSFET. As a TSEP, this work utilizes the MOSFET's forward voltage. Before deriving the thermal resistance, the forward voltage is calibrated by the function of the MOSFET's junction temperature. For this purpose, a sensing current and heating current are applied to the two ends of the MOSFET, which heats up and serves as a heat source. Sequentially, the current flowing through and voltage across the testing MOSFET are measured and calculated to find the power loss of the device, given as

$$P_{loss} = I^2 \times R \quad (2)$$

where I is the drain current and R is the on-resistance of the MOSFET.

For a precise measurement, the thermal resistance was measured using Power Tester 1500A by Mentor Graphics. This machine has a cold plate connected to a thermostat. The cold plate is controllable to have a certain temperature, ranging from −80 °C to 250 °C, by the virtue of the linked liquid cooler. On this temperature-controlled plate, a testing module is placed and its TSEP is calibrated by the method explained above. The TSEP calibration range is determined, considering the environment condition faced by this EPS power module because it is placed on the steering column near the high-temperature engine room.

Figure 6 illustrates the measurement setup. The equipment supports JEDEC standards and directly measured the TSEP
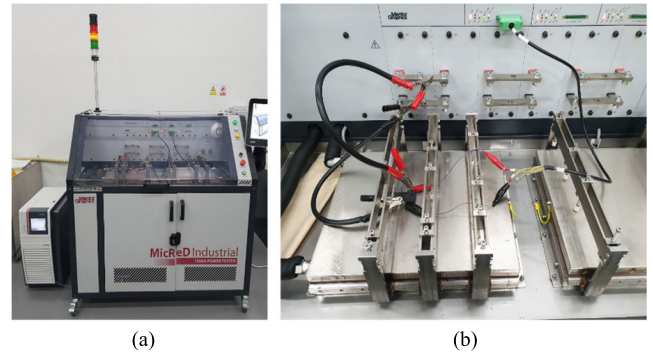
of the device under test (DUT) in the following steps. The DUT was repeatedly turned on and off and continuously heated up and cooled down. By repeating this process, the raw data symbolizing thermal characteristics were obtained, and the thermal properties of the testing module were calculated using thermal modeling via deconvolution and discretization processes. As an example, the measurement results were used to visualize a graph called a structure function representing the Cauer network model of thermal impedance. The derived graph can be used to analyze the thermal resistance of a layer of the power module [30] and, if needed, to monitor its failure symptoms [31], [32].

The designed power module under test is shown in Fig. 6(b). The module was mounted on a cooling plate using thermal grease. The structure function of the module is shown in Fig. 7. The structure function is a graph whose gradient varies depending on the properties and dimensions of the material, and, in the figure, its x-axis is the thermal resistance and y-axis is the thermal capacitance. As the power module is mounted using thermal grease, the point where its gradient changes rapidly are judged to be the thermal resistance of the module. This point is highlighted by the red box, and R_{th} was found to be ∼0.27 K/W. This small R_{th} value was consistent over several repeated measurements. Note that our power module has an exposed copper pattern, and the measured thermal resistance is from the junction to the copper pattern. Our measurement setup is further examined by measuring the R_{th} of a commercial power module, which is found to be almost identical to its datasheet [2].

We employed the measured thermal resistance, R_{th}, as a criterion for determining the accuracy of our simulations. Of course, electrical characteristics are also popularly used as critical factors describing the performance and reliability of a developed power module [32], [33]. However, in this work, it is difficult to perform a one-to-one comparison of the characterized electrical parameters (e.g., $V_{CE(ON)}$ or $R_{CE(ON)}$ values) with the electrical FEM simulation results in Figs. 8 and 11, revealing that parasitic resistance/inductance and current density are converted to volume loss. The thermal resistance is another common indicator representing the performance and reliability of power devices and modules [34].
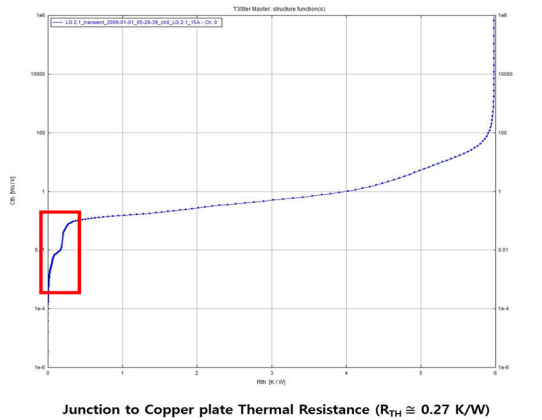
FIGURE 7. Structure function measured for the EPS power module.

FIGURE 8. Uncoupled electrical simulation results showing (a) parasitic resistance and inductance and (b) distribution of volume loss density.

FIGURE 9. Non-iterative thermal simulation results showing the temperature contour plot and location of maximum module temperature.

Moreover, R_{th} can be a representative parameter revealing the multi-physics property because the electrical energy loss of MOSFET devices in our thermal simulations is converted to heat generated from the devices, and heat dissipation is monitored. This process is identical to the functionality of our R_{th} measurement equipment, the Power Tester 1500A.

III. RESULTS AND DISCUSSION

A. INDIVIDUAL AND UNCOUPLED FEM SIMULATIONS

As discussed earlier, electrical, and thermal simulations of power modules have previously been conducted separately. For comparison purposes, conventional FEM simulations were conducted. As power modules build electronic power circuits, such as converters and inverters, the circuit operation is critically affected by the parasitic resistance and inductance of power modules. Thus, the parasitic resistance and inductance of the designed power module were simulated by ANSYS Q3D software and are illustrated in Fig. 8(a). Considering the operating frequency of the MOSFET device used, the switching frequency of these electrical simulations was determined to be 5 MHz, considering the operating frequency and harmonics of the EPS power module. The parasitic resistance and inductance were simulated as 1.1 mΩ and 30.4 nH, respectively. The simulation also provided the current density, which was converted to volume loss density, as depicted in Fig. 8(b).

The thermal FEM simulations utilized ANSYS Icepak software. The volume loss generated from the electrical simulations was applied as a heating source for the thermal simulations. The heating source includes not only the MOSFET power loss but also the loss of the shunt resistors. As our EPS module does not have a liquid or forced-air cooler, its heat dissipation condition is a natural convection with a turbulent flow. In addition, the ambient temperature is set to be 125 °C, which is also used in the experiments in Section II-C, because the EPS module is located close to the engine room. Figure 9 shows the temperature contour of the designed module mounted on its assembly. The maximum temperature of the module was found to be 154.05 °C. Using
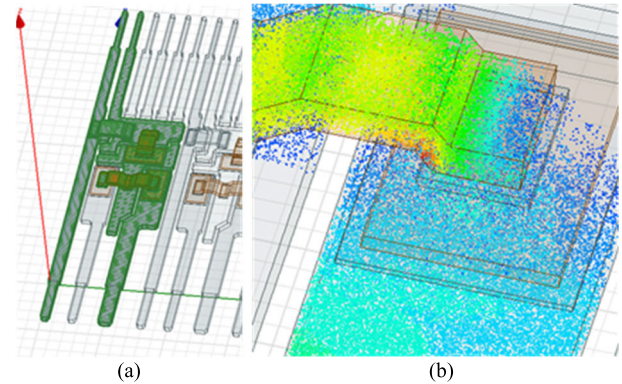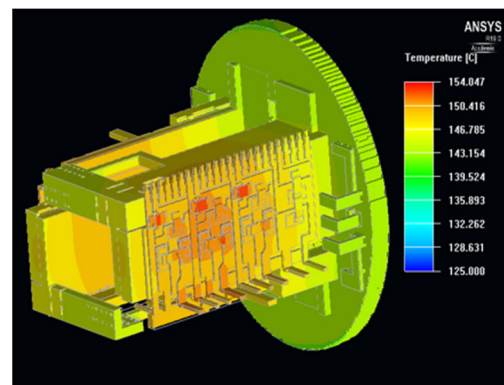
the maximum temperature and temperature distribution of the figure, we calculated the module's thermal resistance. Although the electrical loss was used as an input for the thermal simulation, it was not a fully coupled multi-physics simulation because the thermal simulation results did not influence the electrical parameters.

B. SETUP OF COUPLED ELECTRICAL-THERMAL SIMULATION WITH FEEDBACK ITERATION

Various TSEPs have been reported for power devices, including statistical (e.g., on-state resistance, saturation current, and threshold voltage) and dynamic (e.g., turn-on/off delay and maximum voltage slope) characteristics [35], [36]. Some of these electrical parameters can cause consecutive changes in thermal characteristics, including device and power module temperature, which sequentially alter the TSEPs. These mutual interactions necessitate coupled electrical–thermal simulations with interactive iterations.

Our approach is illustrated in Fig. 10. ANSYS Q3D software simulated the power module model in Fig. 3(a) and extracted electrical properties, including current density and parasitic resistance/inductance. The FEM simulation also generated the volume loss distribution of the power module, which was converted to heating loss. The loss was applied as a boundary condition of the heat source for the thermal
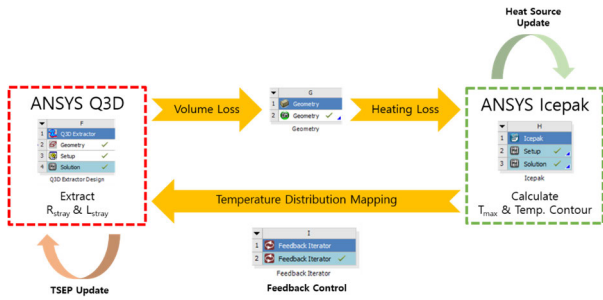
FIGURE 10. Proposed coupled electrical–thermal simulation with iterative feedback functions. The concept was established using the ANSYS Workbench software incorporating ANSYS Q3D, Icepak, and feedback iterator.

FIGURE 11. Electrical simulation results showing volume loss densities derived using (a) the conventional individual, uncoupled, non-iterative method and (b) the proposed coupled electrical–thermal simulation with feedback iterations.

FIGURE 12. Thermal simulation results comparing the temperature distribution contour plots using (a) the conventional individual, uncoupled, non-iterative method and (b) the proposed coupled electrical–thermal simulation with feedback iterations.

simulation conducted by the ANSYS Icepak software, and the temperature distribution contour plot and maximum temperature value were derived. This process is identical to the uncoupled simulation without iteration presented in Section III-A.

The difference is that the temperature distribution is fed to the ANSYS Q3D software by the feedback iterator. For the feedback, it is important to properly select a TSEP. In this study, the on-resistance of the power module was employed because it consists of contributions from both the power devices (on-resistance, $R_{DS(ON)}$) and copper patterns of the substrate (parasitic resistance, R_{Cu}). In addition, both $R_{DS(ON)}$ and R_{Cu} are relatively linear with temperature. This linearity is beneficial in decreasing the computational load and increasing the convergence possibility of the iterative analysis. The MOSFET on-resistance may not be perfectly linear with the temperature, but it can be considered linear within the limited temperature range used in the iterative process of our simulations [36]. Thus, $R_{DS(ON)}$ was expressed as

$$\begin{aligned} R_{DS(ON),2} &= R_{DS(ON),1} \left[1 + \alpha_{DS} \cdot (T_2 - T_1) \right] \\ &= R_{DS(ON),1} \left[1 + \alpha_{DS} \cdot \Delta T \right] \end{aligned} \quad (3)$$

where $R_{DS(ON),1}$ and $R_{DS(ON),2}$ are the on-resistances at temperatures T_1 and T_2, respectively. α_{DS} is the temperature coefficient of resistance (TCR) of the MOSFET on-resistance. Likewise, the parasitic resistance of the copper pattern was expressed as

$$\begin{aligned} R_{Cu,2} &= R_{Cu,1} \left[1 + \alpha_{Cu} \cdot (T_2 - T_1) \right] \\ &= R_{Cu,1} \left[1 + \alpha_{Cu} \cdot \Delta T \right] \end{aligned} \quad (4)$$

where $R_{Cu,1}$ and $R_{Cu,2}$ are the Cu pattern parasitic resistances at T_1 and T_2, respectively. α_{Cu} is the TCR of copper. $R_{DS(ON)}$ and R_{Cu} change according to the temperature at a specific location, and their parasitic inductance and current density are sequentially updated. Using the updated electrical results, the thermal simulation was conducted again. This coupled simulation continued until the variation in its thermal parameters, which are the device temperature herein, converged to less than 1%.

Our feedback iteration tool was implemented in the ANSYS Workbench environment because it contains the
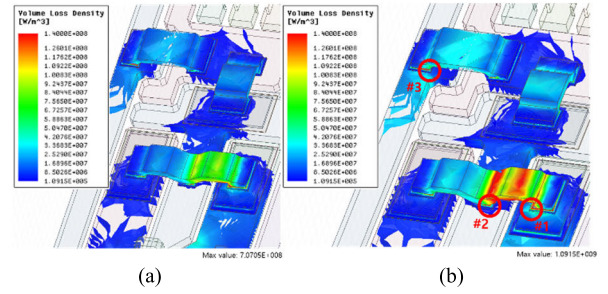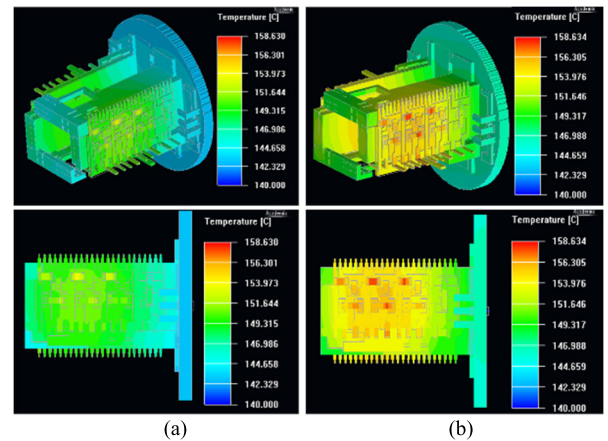
Q3D, Icepak, and feedback iterator as sub-programs. Q3D and Icepak share simulation objects through a modeling tool called Design Modeler, and their results were consequently updated using the feedback iterator.

C. COMPARISON OF SIMULATION RESULTS

Figures 11 and 12 compare the electrical and thermal characteristics with and without the coupled feedback interactions simulations. After five iterations, the coupled simulation results converged, and some of them revealed distinct differences. From the electrical results, the stray inductance of the power module did not change significantly. However, an obvious change in the resistances was observed. For example, the parasitic resistances of the three loops in the three-phase inverter module exhibited an average change from ~1.1mΩ to ~1.6mΩ, which is an approximate increase of 50%, due to the thermal impact. Because of the increased resistance, the two contour plots of volume loss densities in Fig. 11 also differ; the two plots have the same legend scales. The three locations, marked by #1, #2, and #3 in Fig. 11(b), are bonding joints found to have high volume-loss densities. The volume loss increased from 4.4×10^8 W/m³ to 6.5×10^8 W/m³, from 2×10^8 W/m³ to 3×10^8 W/m³, and from 2.7×10^8 W/m³ to 4.3×10^8 W/m³ in #1, #2 and #3,

respectively. At each location, the loss density increased by ∼50%, which is similar to the increase in resistance and is non negligible. The increased loss is additionally expected to heat up the power module.

The simulated temperature distributions are shown in Fig. 12; the legend scales of the temperature plots were adjusted to be identical. The module temperature notably increased with the feedback iterations. Note that the overall temperature increased, even though the maximum temperatures occurred at similar locations. The maximum temperature of the coupled simulation was 158.63 °C, representing an increase of 4.58 °C, because of the increased loss density. The maximum device temperature is lower than the operating junction temperature of the MOSFET [29].

Based on the simulation results, the thermal resistance was calculated using equation (1). It is noteworthy that R_{th} of the coupled simulation was ∼0.26 K/W, which is almost identical to the measurement value (∼0.27 K/W) given in Section II-C, referring that the coupled-simulated and measured junction temperatures are also almost identical. These analysis results demonstrate that the proposed approach is more accurate and reliable than uncoupled simulations for our application and design. Therefore, coupled electrical–thermal simulation with iterations should be employed in power module analyses.

IV. CONCLUSION

Feedback iterated coupled simulation was conducted for a designed power module. The sample module was fabricated and tested to measure its electrical and thermal characteristics. I-V curves and the transfer characteristics were extracted by a curve tracer and a customized jig. The thermal resistance was measured, and the structure function was determined using a power tester. To apply coupled simulation, general electrical and thermal simulations were conducted for the designed power module, which was connected to ANSYS to build a multi-physics simulation environment. The results interacted with each other to increase the parasitic resistance and volume loss density by ∼50% and increase the thermal resistance value by ∼4%. Based on the results of the feedback-iterated coupled simulation, it was demonstrated that more precise and reliable results can be extracted with the proposed approach, and the calculated value of thermal resistance of ∼0.26 K/W was almost identical to the actual measured value of ∼0.27 K/W.

REFERENCES

[1] S. Shin, B. Jin, K. Song, S. Oh, and T. Yim, "Development of new 600 V smart power module for home appliances motor drive application," in *Proc. Int. Exhib. Conf. Power Electron., Intell. Motion, Renew. Energy Manage.*, Jun. 2018, pp. 1–6.

[2] J. Lim, J. Seong, J. Jeon, Y. S. Kim, H.-C. Im, W. S. Hong, and S. W. Yoon, "Design and experimental evaluation of transfer-molded 650 V super-junction MOSFET power module for industrial applications," *IEEE Trans. Ind. Appl.*, vol. 57, no. 6, pp. 6295–6305, Nov. 2021.

[3] Y. Hinata, M. Horio, Y. Ikeda, R. Yamada, and Y. Takahashi, "Full SiC power module with advanced structure and its solar inverter application," in *Proc. 28th Annu. IEEE Appl. Power Electron. Conf. Expo. (APEC)*, Mar. 2013, pp. 604–607.

[4] X. Li, D. Li, G. Chang, M. Packwood, D. Pottage, A. Su, Y. Wang, H. Luo, and G. Liu, "Switching performance of a 3.3-kV SiC hybrid power module for railcar converters," *IEEE Access*, vol. 8, pp. 182600–182609, 2020.

[5] T. Evans, T. Hanada, Y. Nakano, and T. Nakamura, "Development of SiC power devices and modules for automotive motor drive use," in *Proc. IEEE Int. Meeting Future Electron Devices*, Jun. 2013, pp. 116–117.

[6] P. Ning, T. G. Lei, F. Wang, G.-Q. Lu, K. D. T. Ngo, and K. Rajashekara, "A novel high-temperature planar package for SiC multichip phase-leg power module," *IEEE Trans. Power Electron.*, vol. 25, no. 8, pp. 2059–2067, Aug. 2010.

[7] P. Ning, F. Wang, and D. Zhang, "A high density 250 °C junction temperature SiC power module development," *IEEE J. Emerg. Sel. Topics Power Electron.*, vol. 2, no. 3, pp. 415–424, Nov. 2014.

[8] A. Matallana, E. Robles, E. Ibarra, J. Andreu, N. Delmonte, and P. Cova, "A methodology to determine reliability issues in automotive SiC power modules combining 1D and 3D thermal simulations under driving cycle profiles," *Microelectron. Rel.*, vol. 102, Nov. 2019, Art. no. 113500.

[9] J. Seong, S. W. Yoon, S. Park, M. Kim, J. Lim, J. Jeon, and H. Han, "Multi-physics simulation analysis and design of integrated inverter power module for electric compressor used in 48-V mild hybrid vehicles," *IEEE J. Emerg. Sel. Topics Power Electron.*, vol. 7, no. 3, pp. 1668–1676, Sep. 2019.

[10] J. Seong, S. Park, M. K. Kim, J. Lim, H. Han, J. Jeon, and S. W. Yoon, "DBC-packaged inverter power module for integrated motor-inverter design used in 48 v mild hybrid starter-generator (MHSG) system," *IEEE Trans. Veh. Technol.*, vol. 68, no. 12, pp. 11704–11713, Dec. 2019.

[11] D. Li, M. Packwood, F. Qi, Y. Wu, Y. Wang, S. Jones, X. Dai, and G. Liu, "3D multiphysics modelling of high voltage IGBT module packaging," in *Proc. 16th Int. Conf. Electron. Packag. Technol. (ICEPT)*, Aug. 2015, pp. 598–602.

[12] C. Papadopoulos, C. Corvasce, A. Kopta, D. Schneider, G. Pâques, and M. Rahimo, "The influence of humidity on the high voltage blocking reliability of power IGBT modules and means of protection," *Microelectron. Reliab.*, vol. 88, pp. 47–470, Sep. 2018.

[13] K. C. Nwanoro, H. Lu, C. Yin, and C. Bailey, "An analysis of the reliability and design optimization of aluminium ribbon bonds in power electronics modules using computer simulation method," *Microelectron. Rel.*, vol. 87, pp. 1–14, Aug. 2018.

[14] X. Dai, Y. Wang, Y. Wu, H. Luo, G. Liu, D. Li, and S. Jones, "Reliability design of direct liquid cooled power semiconductor module for hybrid and electric vehicles," *Microelectron. Rel.*, vol. 64, pp. 474–478, Sep. 2016.

[15] L. Xu, Y. Liu, and S. Liu, "Modeling and simulation of power electronic modules with microchannel coolers for thermo-mechanical performance," *Microelectron. Rel.*, vol. 54, no. 12, pp. 2824–2835, Dec. 2014.

[16] J. Jeon, J. Seong, J. Lim, M. K. Kim, T. Kim, and S. W. Yoon, "Finite element and experimental analysis of spacer designs for reducing the thermomechanical stress in double-sided cooling power modules," *IEEE J. Emerg. Sel. Topics Power Electron.*, vol. 9, no. 4, pp. 3883–3891, Aug. 2021.

[17] M. Jiang, G. Fu, M. B. Fogsgaard, A. S. Bahman, Y. Yang, and F. Iannuzzo, "Wear-out evolution analysis of multiple-bond-wires power modules based on thermo-electro-mechanical FEM simulation," *Microelectron. Rel.*, vols. 100–101, Sep. 2019, Art. no. 113472.

[18] I. Swan, A. Bryant, P. A. Mawby, T. Ueta, T. Nishijima, and K. Hamada, "A fast loss and temperature simulation method for power converters, Part II: 3-D thermal model of power module," *IEEE Trans. Power Electron.*, vol. 27, no. 1, pp. 258–268, May 2012.

[19] T. M. Evans, Q. Le, S. Mukherjee, I. Al Razi, T. Vrotsos, Y. Peng, and H. A. Mantooth, "PowerSynth: A power module layout generation tool," *IEEE Trans. Power Electron.*, vol. 34, no. 6, pp. 5063–5078, Jun. 2018.

[20] A. Consoli, F. Gennaro, A. Testa, G. Consentino, F. Frisina, R. Letor, and A. Magri, "Thermal instability of low voltage power-MOSFETs," *IEEE Trans. Power Electron.*, vol. 15, no. 3, pp. 575–581, May 2000.

[21] S. Liu, X. Xie, X. Zhang, and W. Zhu, "Analysis of thermal instability in power MOSFET," in *Proc. 3rd Int. Conf. Electron. Inf. Technol. Comput. Eng. (EITCE)*, Oct. 2019, pp. 541–545.

[22] Z. Wang, X. Shi, L. M. Tolbert, F. Wang, Z. Liang, D. Costinett, and B. J. Blalock, "Temperature-dependent short-circuit capability of silicon carbide power MOSFETs," *IEEE Trans. Power Electron.*, vol. 31, no. 2, pp. 1555–1566, Feb. 2016.

[23] R. Wu, H. Wang, K. B. Pedersen, K. Ma, P. Ghimire, F. Iannuzzo, and F. Blaabjerg, "A temperature-dependent thermal model of IGBT modules suitable for circuit-level simulations," *IEEE Trans. Ind. Appl.*, vol. 52, no. 4, pp. 3306–3314, Jul./Aug. 2016.

[24] H. Cao, P. Ning, X. Wen, T. Yuan, and H. Li, "An electrothermal model for IGBT based on finite differential method," *IEEE J. Emerg. Sel. Topics Power Electron.*, vol. 8, no. 1, pp. 673–684, Mar. 2020.

[25] L.-L. Liao, T.-Y. Hung, C.-K. Liu, W. Li, M.-J. Dai, and K.-N. Chiang, "Electro-thermal finite element analysis and verification of power module with aluminum wire," *Microelectron. Eng.*, vol. 120, pp. 114–120, May 2014.

[26] D. Lee, K.-S. Kim, and S. Kim, "Controller design of an electric power steering system," *IEEE Trans. Control Syst. Technol.*, vol. 26, no. 2, pp. 748–755, Mar. 2018.

[27] X. Ma, Y. Guo, and G. Liu, "Automobile EPS temperature observation method based on extended state observer," *J. Franklin Inst.*, vol. 355, no. 18, pp. 9108–9126, Dec. 2018.

[28] Y. Liu, Y. Xu, and Y. Liu, "Reliability modeling analysis of a power module," in *Proc. 14th Int. Conf. Thermal, Mech. Multi-Physics Simul. Experiments Microelectron. Microsystems (EuroSimE)*, Apr. 2013, pp. 1–11.

[29] *Automotive N-Channel 40 V 175°C MOSFET (SQC40022E)*, Vishay, Malvern, PA, USA, 2018.

[30] F. N. Masana, "A new approach to the dynamic thermal modelling of semiconductor packages," *Microelectron. Rel.*, vol. 41, no. 6, pp. 901–912, Jun. 2001.

[31] M. A. Eleffendi, L. Yang, P. Agyakwa, and C. M. Johnson, "Quantification of cracked area in thermal path of high-power multi-chip modules using transient thermal impedance measurement," *Microelectron. Rel.*, vol. 59, pp. 73–83, Apr. 2016.

[32] M. A. Eleffendi and C. M. Johnson, "In-service diagnostics for wire-bond lift-off and solder fatigue of power semiconductor packages," *IEEE Trans. Power Electron.*, vol. 32, no. 9, pp. 7187–7198, Sep. 2017.

[33] C. Chen, V. Pickert, M. Al-Greer, C. Jia, and C. Ng, "Localization and detection of bond wire faults in multichip IGBT power modules," *IEEE Trans. Power Electron.*, vol. 35, no. 8, pp. 7804–7815, Aug. 2020.

[34] L. R. GopiReddy, L. M. Tolbert, and B. Ozpineci, "Power cycle testing of power switches: A literature survey," *IEEE Trans. Power Electron.*, vol. 30, no. 5, pp. 2465–2473, May 2015.

[35] Y. Avenas, L. Dupont, and Z. Khatir, "Temperature measurement of power semiconductor devices by thermo-sensitive electrical parameters—A review," *IEEE Trans. Power Electron.*, vol. 27, no. 6, pp. 3081–3092, Jun. 2012.

[36] L. Zhang, P. Liu, S. Guo, and A. Q. Huang, "Comparative study of temperature sensitive electrical parameters (TSEP) of Si, siC and GaN power devices," in *Proc. IEEE 4th Workshop Wide Bandgap Power Devices Appl. (WiPDA)*, Nov. 2016, pp. 302–307.

JANGMUK LIM received the B.S. degree in automotive engineering from Hanyang University, Seoul, Republic of Korea, in 2016, where he is currently pursuing the Ph.D. degree in automotive engineering. His current research interests include analysis and design about power module for reliability improvement.

JAEJIN JEON received the B.S. degree in mechanical engineering from Dongguk University, Seoul, South Korea, in 2016. He is currently pursuing the Ph.D. degree with the Department of Automotive Engineering, Hanyang University, Seoul. His research interests include cover thermal stress of solder joints and cooling methods in power module package.

JIHWAN SEONG received the B.S. degree in automotive engineering from Hanyang University, Seoul, Republic of Korea, in 2015, where he is currently pursuing the Ph.D. degree in automotive engineering. His research interests include power module package and reliability analysis.

JAEHYUN CHO received the B.S. degree in mechanical engineering, Ajou University, Suwon, South Korea, in 2016. He is currently pursuing the M.S. degree with the Department of Automotive Engineering, Hanyang University, Seoul. From 2017 to 2020, he was a Mechanical Designer at vehicle parts companies. His research interests include power module encapsulation process and its reliability.

SEONG MOO CHO received the B.S. and M.S. degrees in electronic and electrical engineering and computer science from Hanyang University, Ansan, South Korea, in 2004 and 2006, respectively, where he is currently pursuing the Ph.D. degree with the Department of Automotive Engineering. He has been engaged as a Research Engineer at LG Electronics Inc. His research field is automotive power module for hybrid and electric vehicles. To be specific, his current research interests include advanced power semiconductor, traction power inverter module, and integrated cooling systems.

KWANG SOO KIM received the B.S. degree in materials science and engineering from the Korea Advanced Institute of Science and Technology, Daejeon, South Korea, in 2004, and the Ph.D. degree in materials science and engineering from the University of Illinois at Urbana–Champaign, Champaign, IL, USA, in 2009. In 2009, he joined Samsung Electro-Mechanics, Suwon, South Korea, where he developed power modules for home appliances and industrial applications. From 2016 to 2020, he was a Principal Engineer at LG Electronics Inc., Seoul. He researched and developed power module products for automotive and industrial applications. Since 2020, he has joined Texas Instruments, Santa Clara, CA, USA, as a Member Group of technical staff (MGTS). He has authored over 40 publications and holds 154 patents. His research interests include high power module package design, simulations, processes and materials for industrial, automotive, and aerospace applications.

SANG WON YOON (Senior Member, IEEE) received the B.S. degree in electrical engineering from Seoul National University, Seoul, South Korea, in 2000, and the M.S. and Ph.D. degrees in electrical engineering and computer science from the University of Michigan, Ann Arbor, MI, USA, in 2003 and 2009, respectively. From 2009 to 2013, he was a Senior Scientist and a Staff Researcher with the Toyota Research Institute of North America, Ann Arbor, where he conducted research in the fields of power electronics and sensor systems for automobiles. Since 2013, he has been with the Department of Automotive Engineering, Hanyang University, Seoul, where he is currently an Associate Professor. His current research interests include power electronics, sensors and sensor systems, electronic reliability, and their applications in conventional and future vehicles.

● ● ●